Lab on a Chip

PAPER

View Article Online
View Journal | View Issue

Cite this: *Lab Chip*, 2014, **14**, 1198

A microfluidic platform for chemoresistive testing of multicellular pleural cancer spheroids†

Janine Ruppen,[ab] Lourdes Cortes-Dericks,[cd] Emanuele Marconi,[a] Golnaz Karoubi,[cd] Ralph A. Schmid,[cd] Renwang Peng,[cd] Thomas M. Marti[cd] and Olivier T. Guenat*[ace]

Received 25th September 2013,
Accepted 25th December 2013

DOI: 10.1039/c3lc51093j

www.rsc.org/loc

This study reports on a microfluidic platform on which single multicellular spheroids from malignant pleural mesothelioma (MPM), an aggressive tumor with poor prognosis, can be loaded, trapped and tested for chemotherapeutic drug response. A new method to detect the spheroid viability cultured on the microfluidic chip as a function of the drug concentration is presented. This approach is based on the evaluation of the caspase activity in the supernatant sampled from the chip and tested using a microplate reader. This simple and time-saving method does only require a minimum amount of manipulations and was established for very low numbers of cells. This feature is particularly important in view of personalised medicine applications for which the number of cells obtained from the patients is low. MPM spheroids were continuously perfused for 48 hours with cisplatin, one of the standard chemotherapeutic drugs used to treat MPM. The 50% growth inhibitory concentration of cisplatin in perfused MPM spheroids was found to be twice as high as in spheroids cultured under static conditions. This chemoresistance increase might be due to the continuous support of nutrients and oxygen to the perfused spheroids.

1. Introduction

To further improve the effectiveness of cancer therapies, it is widely believed that tumors should be considered in their three-dimensional (3D) structure because cells can attain increased resistance under those conditions.[1] This phenomenon known as multicellular resistance[2] may not be fully reflected in two-dimensional (2D) cell cultures.[3] Therefore, 3D cell culture models, such as spheroids, better reflect the *in vivo* behavior of cells in tumor tissues and are excellent surrogates to predict tumorigenic potential *in vivo*.[4–6] Hence, multicellular spheroids are becoming an important tool in cancer research by representing a 3D system of intermediate cellular complexity between monolayer cell cultures and *in vivo* tumors.[2] However, spheroids cultured in standard well plates still do not fully reflect the *in vivo* conditions of the tumors, in particular because in such a system, the spheroids are immerged in a static solution of physiological medium rather than being perfused, like *in vivo* vascularized tumors. Microfluidic platforms that can easily mimic the geometrical shape and the dynamic microenvironment of capillaries are ideally suited to mimic this aspect. The greatest benefit of such perfused systems is the ability to preserve steady-state environments where fresh medium and oxygen flow in and waste products are removed, such as in the *in vivo* environment. Perfused microfluidic systems also provide a more physiologically accurate model of drug exposure and mass transport to cultured cells.[7–9] During the last decade, microfluidic technologies have also demonstrated their ability to accurately manipulate cells and tissues with unprecedented spatiotemporal precision.[9,10] In parallel with ongoing developments in cellular and molecular biology, these microfluidic systems are expected to significantly contribute to the advancement of anti-cancer strategies and are thought to represent the platform of choice for the next-generation of *in vitro* cancer models.[11]

Although only just emerging, microfluidic platforms for spheroid cultivation and anti-cancer drug testing have already demonstrated great potential.[12] These systems allow for the growth of spheroids of homogeneous sizes and for the subsequent exposure to specific chemotherapeutical treatments. The cytotoxic responses to drugs are mostly quantified using morphology and fluorescent imaging[13] or confocal microscopy.[14–18] The latter technique is rather time-consuming, particularly for

[a] *ARTORG Lung Regeneration Technologies Lab, University of Berne, Murtenstrasse 50, CH-3010 Berne, Switzerland. E-mail: olivier.guenat@artorg.unibe.ch; Fax: +41 31 632 7576; Tel: +41 31 632 7608*
[b] *Graduate School for Cellular and Biomedical Sciences, University of Berne, Switzerland*
[c] *Division of General Thoracic Surgery, University Hospital of Berne, Berne, Switzerland*
[d] *Department of Clinical Research, University of Berne, Berne, Switzerland*
[e] *University Hospital of Berne, Division of Pulmonary Medicine, Berne, Switzerland*

† Electronic supplementary information (ESI) available: Caspase-3/7 activity comparison with and without cells, caspase-3/7 activity comparison between 2D and 3D cultures as well as between 2D and 3D perfused cultures, and a video showing spheroid loading on chip. See DOI: 10.1039/c3lc51093j

spheroids, for which several cell layers must be analyzed. Cell viability in spheroids is also demonstrated using scanning electrochemical microscopy (SECM)[19] as well as by evaluating the fluorescence following conversion of alkoxyresorufin to resorufin.[20] Recently, Kim and colleagues designed a cell viability assay on chip derived from a standard 2D viability assay, particularly the MTT ((3-4,5-dimethylthiazol-2-yl)2,5-diphenyltetrazolium bromide) assay.[21] However, this rather complex microfluidic system requires a number of valves allowing for successive and precise microfluidic operations.

In this study, we propose a new microfluidic chemosensitive platform for spheroid testing based on a simple and fast analysis system: the collection of the supernatant from the spheroid cultured on chip and its further analysis using a standard plate reader. In contrast to the time-demanding confocal microscopy and the associated image analysis, this technique is very fast and straightforward. We chose to assess apoptosis in response to the chemotherapeutic insult based on the caspase-3 activity collected in the spheroid supernatant. These assays were performed using a limited number of spheroids each made up of a small number of cells in the perspective of personalized medicine applications.

As a proof of concept, malignant pleural mesothelioma (MPM) cell lines were tested on this platform. MPM is a rare, but highly aggressive and lethal, thoracic cancer with increasing incidence throughout the world. This therapy-resistant neoplasm is associated with exposure to asbestos in 60–70% of cases[22,23] and is characterized by a locally aggressive growth pattern in the lower parietal pleura with subsequent metastasis as the disease progresses.[24] The patients' survival time after surgery averages 14 months.[25] The standard chemotherapeutical approach consists of a combination of cisplatin and pemetrexed. In this study, the MPM spheroids are exposed to cisplatin and their chemoresistances in a static and a dynamic environment are compared. To the best of our knowledge, this is the first time that the influence of perfusion on the chemoresistance of spheroids is reported.

2. Materials and methods

2.1. Spheroid formation and growth

All cell manipulations were performed in a sterile flow hood and cells were incubated at 37 °C and 5% CO_2 except if otherwise stated. Cells, obtained from the human mesothelioma cell line H2052 (ATCC-CRL-5915, ATCC, France), were maintained in RPMI1640 (Invitrogen) media containing 10% fetal bovine serum, FBS (Sigma) and 1% of a mixture of penicillin and streptomycin (P–S, Invitrogen). Cells were passaged twice a week using 0.25% trypsin with EDTA (Gibco) and counted using Trypan blue staining and a hemocytometer (bright-line Neubauer improved). Monolayer cell cultures were established in 96-well plates with a density of 50 cells mm^{-2}.

For spheroid formation, H2052 cells were seeded in a 24 ultra-low attachment flat-bottom well plate (Corning, Sigma) at a density of 53 cells mm^{-2}. Cells were maintained in RPMI1640 media supplemented with 20 ng ml^{-1} of epidermal growth factor, EGF (Gibco, Invitrogen), 20 ng ml^{-1} of basic fibroblast growth factor, bFGF (Gibco, Invitrogen), 4 μg ml^{-1} of insulin (BioReagent, Sigma), 2% serum-free supplement B27 (Gibco, Invitrogen) and 0.5% P–S. During the three days of culture in media supplemented with growth factors, several spheroids formed spontaneously. The spheroids, the sizes of which varied between 50 and 400 μm, were filtered using a 40 μm nylon cell strainer (BD Falcon, Switzerland) to eliminate single cells that did not spontaneously form spheroids. All the filtered spheroids were trypsinized (TrypLE Express (1×), LubioScience, Invitrogen) and incubated for 12 minutes to disaggregate spheroids into single cells. The reason why the spontaneously formed spheroids were not size sorted at 160 μm is due to the small percentage (5–10%) of spheroids obtained in this size. After stopping the reaction with RPMI1640 containing 2% B27 and 0.5% P–S and four minute centrifugation at 200 rcf, 200 cells (6 cells mm^{-2}) were seeded in each well of a non-tissue culture-treated 96 U-bottom well plate (BD Falcon) and centrifuged at 515 rcf at room temperature (RT) for 10 minutes (ref. 26) before being incubated for 48 hours.

2.2 Design and fabrication of the microfluidic platform

The spheroid trapping principle used on the microfluidic platform is based on a serial entrapment for beads,[27] which we recently tested successfully on a device in which 500 μm in diameter ovarian cancer spheroids[17] were trapped and exposed to chemotherapeutic drugs. The microfluidic chip comprises two identical channels, each equipped with eight trapping sections, each for one spheroid (Fig. 1A).

Briefly, the trapping principle works as follows: when the chip is empty, the hydraulic resistance along the trapping channel is lower than the hydraulic resistance of the bypass channel. Thus, when a first spheroid is loaded on the chip, it will follow the path of least resistance and will be kept in the trapping section (Fig. 1B). The spheroid then acts as a plug, increasing the hydraulic resistance of the trapping channel and redirecting the main flow to the bypass channel (Fig. 1C). The next spheroid loaded on the chip is trapped in the second trapping section similar to the first one until all eight traps are filled with spheroids.

Given the desired size of the spheroids to be tested on chip, the hydraulic resistance (R_h) ratio between the trapping section and the bypass channel is calculated using the Hagen–Poiseuille equation $\Delta p = R_h Q$, with:

$$R_h = \frac{128 \times \mu \times l}{\pi \times D_h^{\,4}} \quad (1)$$

where μ is the dynamic viscosity of the physiological medium, l the channel length, and D_h the hydraulic diameter of the channel with a rectangular cross-section. The microfluidic channels are designed so that the ratio between the flow through the trapping channel (Q_T) and the flow through the bypass channel (Q_B) is equal to 1.8. The hydraulic resistance remains higher in the bypass channel when no spheroid is trapped.

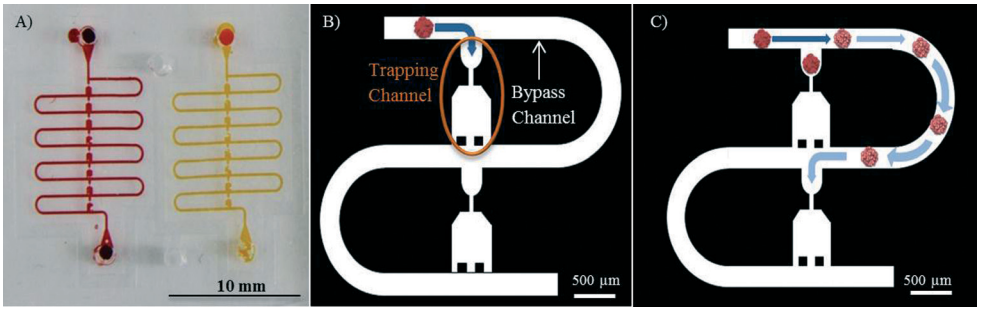

Fig. 1 A) A picture of the entire microfluidic system with 2 channels for spheroid testing (red for the chemotherapeutical drug treatment and yellow for control). B) Schematic of the trapping principle: the first spheroid follows the fluidic path with the smallest fluidic resistance and falls in the first trap. C) Once a spheroid is trapped, the flow resistance of the first trapping channel becomes larger than that of the bypass channel, redirecting the flow with the second spheroid to the bypass channel until the next empty trap.

All of the microchannels are 200 μm high and 200 μm wide, except in the trapping channel. The latter is composed of three different sections. The first consists of a spheroid trap with a width of 200 μm and a length of 300 μm. The second section is a 50 μm wide and 150 μm long narrow channel, whereas the last part is a 500 μm × 500 μm × 200 μm channel with two cuboids (100 μm × 100 μm × 200 μm) aligned horizontally at the end of the channel to guide the spheroids along the main channel. The two cuboids are spaced by 100 μm and are located 100 μm from the border (Fig. 1B).

The devices were fabricated with poly(dimethylsiloxane) (PDMS) (Sylgard 184, Dow Corning) using soft lithography techniques. Briefly, a silicon mold made from a 4″ silicon wafer was microstructured with 200 μm deep microchannels using deep reactive-ion etching (DRIE). Each silicon master allowed simultaneous molding of seven PDMS devices. The actual channel dimensions on the master were 205 ± 2 μm in width and 205 ± 2 μm in depth. In the final step, the micromolded PDMS part was bonded to a microscopy glass slide using oxygen plasma.

2.3. Spheroid loading on the microfluidic platform

Prior to the spheroid loading, the microchannels were successively rinsed under sterile conditions with isopropanol, 70% ethanol and deionized water. To prevent spheroid adherence to the microchannels, a 100 μl solution of synperonic F-108 (1% w/v, Fluka, Sigma) was introduced in the chip and incubated for 60 minutes. RPMI1640 containing 2% serum-free supplement B27 and 0.5% P–S was then flashed twice into the microchannels. The outlets of the chip were connected under sterile conditions using Teflon tubes (ID = 0.6 mm) to a 2 ml cryo vial (VWR International, Switzerland), allowing for the collection of the supernatants. The loading of the spheroids was performed using a 100 μl pipette tip containing eight spheroids which was placed at the inlet. After trapping of the spheroids, the two channels of the chip were connected to a syringe pump (Harvard Apparatus) equipped with two 1 ml syringes, and then perfused either with media or with media containing cisplatin. Once trapped, the spheroids close the small trapping channels and are thus cultured in a diffusion driven transport system.

Spheroids were perfused under sterile conditions at 37 °C and 5% CO_2 with a flow rate of 0.1 μl min^{-1} for 48 hours. The supernatant used for the cell viability test was sampled during the whole assay period.

The spheroid loading on the chip (see video in the ESI†) was observed using a small microscope placed in the incubator (JuLI smart fluorescent cell analyzer). The spheroid morphology was visualized under perfusion every 10 minutes using the same microscope.

2.4. Chemosensitivity assays

Two methods were used for comparison purposes to assess the 50% growth inhibitory concentration (GI50) of cisplatin: the XTT assay and the Caspase-Glo® 3/7 assay. The cell mortality in monolayer cultures (2D) as well as in spheroids cultured under static (3D) or perfused (3D on chip) conditions was assessed using different concentrations of cisplatin (2 μM, 4 μM, 8 μM, 16 μM, 32 μM, 64 μM, 96 μM, 128 μM, 192 μM, 256 μM). For this purpose, cisplatin (0.5 mg ml^{-1}, Sandoz) was diluted in either RPMI1640 media containing 10% FBS and 1% P–S for 2D cultures or RPMI1640 media containing 2% B27 and 0.5% P–S for 3D cultures. The growth factors were removed from the physiological medium used for the 3D cultures in order to keep the spheroid size constant and avoid the presence of a necrotic core. Staurosporine at a concentration of 1 μM was used as the positive control. All experiments were done at least in triplicate and over a time period of 48 hours.

2.5. Analysis of apoptosis in multicellular spheroids

2.5.1 Immunostaining and fluorescence imaging: Hoechst/PI. Hoechst/PI staining was performed on the spheroids to assess their viability after the loading process. For the 3D cultures on chip, 100 μl of Annexin-V-Fluos labelling solution with 1 μg ml^{-1} of Hoechst33342 was introduced in the chip and incubated for 20 minutes. Then, fresh medium was flashed through the chip to eliminate background signals from the staining. Microscopic

pictures were taken using an inverted Leica DMI4000B fluorescent microscope with a CCD camera (Leica DFC360 FX). The pictures were processed using the Leica AF image analysis software and further processed and visually analyzed using the Fiji image analysis software based on ImageJ (http://rsbweb.nih.gov/ij/).

2.5.2 XTT assay. The XTT (Cell Proliferation Kit II, Roche) assay was only performed for the monolayer cultures. 50 cells mm^{-2} were seeded in triplicate in a 96-well flat-bottom microplate (BD Falcon) and incubated overnight to allow cell attachment. After 48 hours of treatment with different concentrations of cisplatin, the medium was aspirated and the cells replenished with 100 μl of fresh medium and 50 μl of XTT labelling mixture. After four hours of incubation, absorbance was measured at a wavelength of 480 nm and a reference wavelength of 650 nm using a multiwell plate reader (TECAN Infinite M1000).

2.5.3 Active caspase-3/7 assay. For the 2D cell cultures, 50 cells mm^{-2} were seeded in triplicate in a 48-well plate (BD Falcon) and incubated overnight to allow cell attachment. After 48 hours of treatment with different concentrations of cisplatin, the supernatant was collected and mixed with Caspase-Glo® 3/7 reagent (Promega) in a 1 : 1 ratio. After 3 hours incubation at RT, luminescence was measured using a TECAN Infinite M1000 reader.

For the 3D cell cultures, eight spheroids were seeded in triplicate in a non-treated, flat-bottom 48-well plate and treated for 48 hours with cisplatin. The Caspase-Glo® 3/7 assay was directly added to each well in a 1 : 1 ratio. After 3 hours incubation at RT, luminescence was measured using a TECAN Infinite M1000 reader.

For the perfused 3D cell culture system, eight spheroids were loaded on the microfluidic device and perfused with cisplatin for 48 hours with a flow rate of 0.1 μl min^{-1}. Supernatants were collected during the whole period of the experiments. The analysis of the supernatants was performed identically as for the supernatants of the 2D cell cultures described above.

2.6. Statistical analysis

Prism6 (GraphPad Software, Inc., Ja Jolla, CA) was used for statistical analysis. The statistical significance was set at a value of 0.05 or lower.

3. Results and discussion

MPM spheroids loaded on the microfluidic platform were grown in non-adherent cultures in order to increase the probability to include tumor initiating cells (TIC) in the spheres. TICs are known to present an increase chemoresistance and are thought to be responsible for tumor recurrence,[1] making them a specific target of chemotherapeutical treatments. Spheroid formation in non-adherent cultures has been used as a surrogate *in vitro* method for detecting TIC from primary human tumors, as recently reviewed by Valent *et al.*[28] The presence of TICs was also recently reported in cell lines,[29] including H2052 MPM cells.[30] Therefore, H2052 spheroids were first cultured in an ultra-low attachment flat-bottom well plate,[31] in which spheroids spontaneously formed. After the filtration of all single cells the remaining spheroids with diameters varying between 50 and 400 μm were disaggregated and seeded in a 96 U-bottom well plate where they formed spheroids with a size distribution shown in Fig. 2A. The larger spheroids were then collected and used for the experiments either on chip or in a standard well-plate. The loading of the formed spheroids on chip, rather than creating spheroids on chip from suspended cells, allowed a strict comparison between the static and the dynamic culture conditions of the identically cultured spheroids.

3.1. Spheroid growth

The spontaneous formation of the spheroids from the suspended cells led to spheres, with a size distribution similar to a Gaussian curve. The uniformity of the spheroid sizes was analyzed by measuring a total of 126 spheroids after 3 days of culture (Fig. 2A). Almost 36% of the spheroids had a size comprised between 160 and 180 μm in diameter, 24% between 140 and 160 μm, 17% between 180 and 200 μm, 14% between 120 and 140 μm, 5.5% between 100 and 120 μm, and 4% were found to

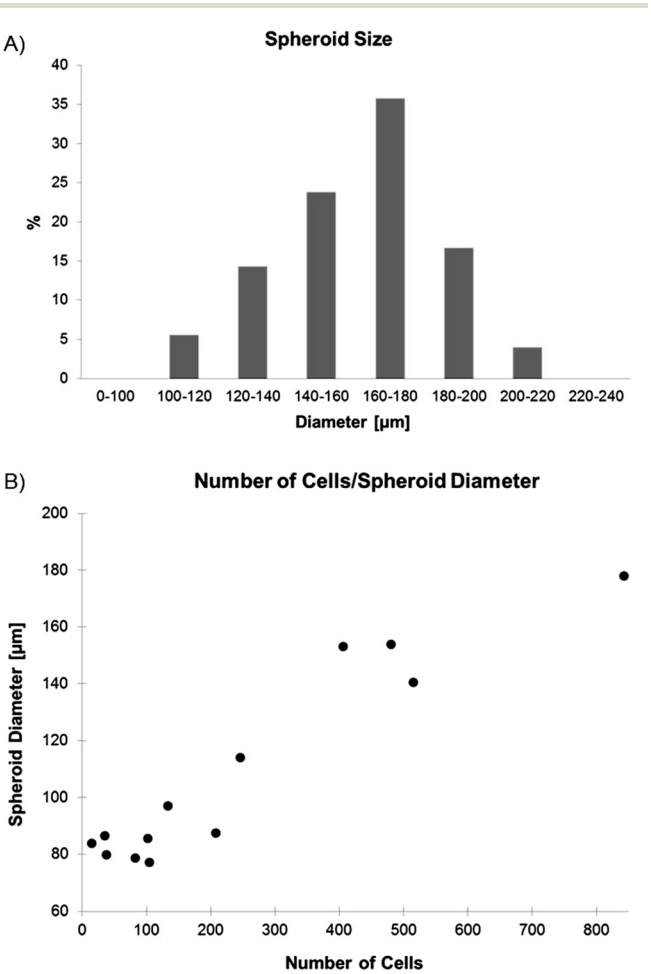

Fig. 2 A) Distribution of the spheroid size obtained in the U-bottom well plate (n = 126). B) Correlation between the spheroid size and the number of cells per spheroid (n = 13).

have a size comprised between 200 and 220 μm. The average size of the obtained spheroids was found to be 161.1 ± 22.7 μm. The number of cells per spheroid was counted in 13 trypsinized spheroids (Fig. 2B). The number of cells of a 160 μm in diameter spheroid used for the chemosensitivity assays was around 550 to 600 cells.

3.2. Trapping and culture of spheroids on chip

The spheroids loaded on the chip were trapped using the difference in flow resistances between the trapping channel and the bypass channel (see video in the ESI†). Once all eight spheroids were trapped, they were perfused for 48 hours. As illustrated in Fig. 3, the morphology of the spheroids stayed unchanged during the whole perfusion period. It should be mentioned that once the spheroids are trapped, the flow that passes in the trapping section is negligible or even non-existent. Therefore, the spheroids are not exposed to shear stress. In fact, the delivery of the nutrients and of the oxygen contained in the physiological medium is essentially due to diffusion from the main channel to the trapped spheroids. This is obviously also true in the other direction, for the cytokines and the cellular waste products that are released by the spheroids.

The spheroids were then stained with Hoechst/PI to analyze their cell viability in their dynamic environment and to prove that spheroids did not develop a necrotic core, which is normally established at sizes larger than 500 μm.[1] The cell mortality was found to be about 10% (data not shown), which coincides with the normal cell mortality found in standard cell cultures. Thus, one can conclude that this microfluidic environment does not affect the cell viability.

3.3 EdU proliferation assay

Cisplatin induces DNA intra- and inter-strand crosslinks, which lead to the inhibition of DNA replication and, as a consequence, to the death of the cells.[32] Therefore, cisplatin affects primarily proliferating cells and, to a lesser extent, arrested cells in the G1 phase of the cell cycle. The proliferative activity of the spheroids was therefore tested using a proliferation assay based on 5-ethynyl-2′-deoxyuridine (EdU), a nucleotide analogue that is incorporated during DNA replication. Our analysis revealed that EdU incorporation was reduced from 44% to 13% in 3D *versus* 2D culture under control conditions at the beginning of the 48 hour treatment (Fig. 4). BrdU incorporation in human lung cancer biopsies was reported to be about 10%,[33] confirming that the 3D model is more relevant for studying how cisplatin affects the survival of cancer cells. Furthermore, the proliferative activity is higher at the beginning of the 48 hour treatment than after the treatment, even under control conditions. In 2D samples, the EdU incorporation decreases from 44 to 25% and in 3D samples from 13 to 7%. This decrease indicates that cells down-regulate their replication with the decrease of nutrients to survive starvation for as long as possible and therefore are more resistant to cisplatin treatment. Moreover, the cell culture reaches confluence and therefore replication is down-regulated. Surprisingly, we observed a 17% increase of EdU incorporation in spheroids treated with 4 μM cisplatin compared to spheroids under control conditions. This increase may be explained by the activation of DNA repair mechanisms and cell proliferation as a result of the cisplatin assault at low concentration. This concentration is too low to kill the cells but may be high enough to damage them by activating their defense mechanisms. This includes cell proliferation and DNA repair mechanisms.

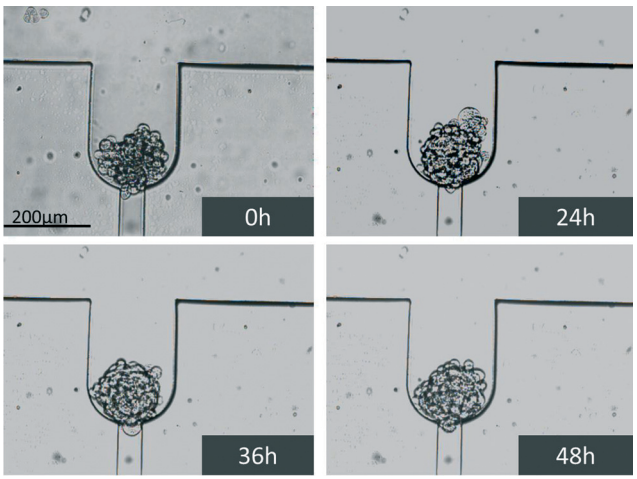

Fig. 3 Bright field images of a spheroid trapped and perfused on chip with control media. The images were taken at the beginning of the perfusion as well as after 24, 36 and 48 hours of perfusion.

3.4. Chemosensitivity assays on chip

Cisplatin penetrates in the spheroids by diffusion and binds with DNA to form inter- and intra-strand crosslinks. Cisplatin is a small molecule that has been shown to diffuse in about 40 min in 280 μm spheroids.[34] In our case, the spheroids are smaller, meaning that the steady state is reached earlier and that this time is negligible in comparison to the 48 h of perfusion.

The GI50 values for the 2D cultures were obtained using the XTT assay and the caspase activity assay for comparison purposes, whereas the GI50 of the 3D cultures were only tested using the caspase activity assay.

3.4.1 XTT assay. The XTT assay, which is based on the measurement of the activity of cellular enzymes that reduce the tetrazolium dye, is one of the golden standards used to assess cell viability. However, its use on chip is somewhat complicated because it requires several manipulations.[21] We used it for the 2D model as a reference assay to validate the caspase-3/7 assay that was used for the cell supernatant. The GI50 of cisplatin for the 2D model (Fig. 5) was 11 μM after 48 hours of exposure. This result corresponds to the value obtained by Cortes-Dericks *et al.*[30] The effect of cisplatin on the cells was further studied to discriminate the inhibition of the cell growth from the cell death. Therefore, the metabolic activity of cells in the control samples at day 0 (*i.e.* before starting the treatment) was measured and used as the reference point.

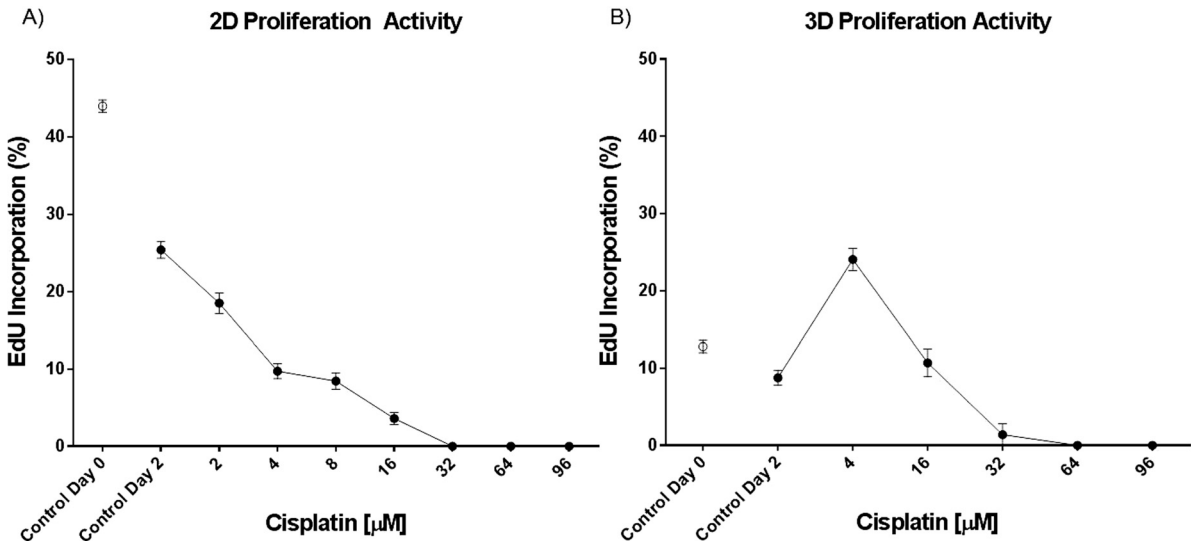

Fig. 4 EdU incorporation in H2052 A) monolayer ($n \geq 8$) and B) spheroid cultures ($n \geq 6$). Data are presented as means ± SEM.

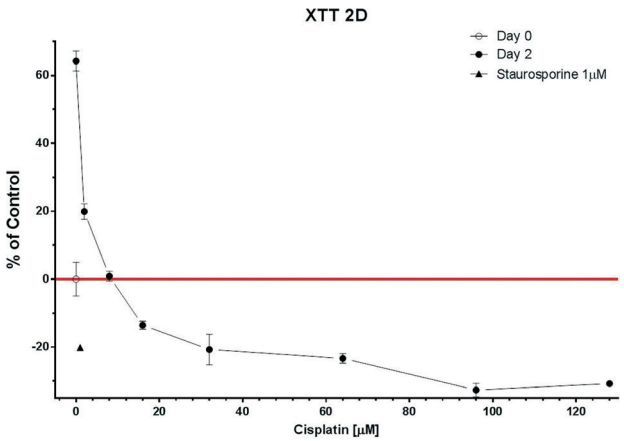

Fig. 5 The XTT assay in 2D cultures (n = 12). Measurements were done at the beginning of the experiment (day 0) and at the end (day 2). 1 μM staurosporine was used as the negative control. Data are presented as means ± SEM.

As illustrated in Fig. 5, cell growth was inhibited in all samples with a metabolic activity higher than this reference point, whereas in the samples with a lower cellular metabolic activity, cisplatin killed the cells. In this assay, the growth inhibition/cell death limit for cisplatin was found to be 32 μM.

3.4.2 Caspase-3/7 assay. The caspase-3/7 activity appears during the last steps of apoptotic cell death and was assessed by the Caspase-Glo® 3/7 assay. This assay is very sensitive and can be used even with a very small number of cells. The test was first evaluated using the supernatant only and then compared with samples containing spheroids. The caspase-3/7 activity was found to be slightly lower in samples with the supernatant compared to samples containing spheroids (Fig. 7 S1, ESI†). However, both curves are comparable and give a similar GI50 response. The slight difference might indicate that a small fraction of the caspase proteins remains in the spheroids and is not collected in the supernatant. No GI50 values were reported so far to the best of our knowledge for H2052 spheroids exposed to cisplatin. Although GI50 values are cell-type dependent, similar values were obtained for non-small cell lung carcinoma cell lines H460 and A549 exposed to cisplatin. In the 3D culture, they were 84 μM (H460) and 75 μM (A549), whereas in the 2D culture, the IC50 values for these two cell lines were around 4 μM.[35]

In addition, the GI50 for the 2D culture obtained using the Caspase-Glo® 3/7 assay (20 μM) was similar to that using the XTT test (14 μM) confirming the validity of the caspase method. The Caspase-Glo® 3/7 assay was further used to characterize the spheroid models. As expected, the chemoresistance of the 3D model (54 μM) was found to be higher than that of the 2D model (20 μM) (Fig. 8 S2, ESI†).

However, the most interesting result was the two-fold chemoresistance increase observed between the 3D and the 3D perfused model (Fig. 6). This increase might be due to the enhanced and continuous support of nutrients and oxygen to the perfused spheroids predicted by Hu *et al.* in a theoretical model.[36] It should be pointed out that the caspase-3/7 activity under the 3D static conditions was measured directly in the wells containing the spheroids and not only in the supernatant. This prevented false positive results due to multipipetting steps. Interestingly, the caspase-3/7 activity suddenly decreased above a certain cisplatin concentration. This peak indicates the highest level of apoptotic cells in the spheroids. Subsequently, the caspase-3/7 activity decreased with the increase of the drug concentration as a result of natural enzyme degradation and cisplatin toxicity, which leads to cell necrosis instead of apoptosis (private communication with Dr. Dan Lazar, Promega).

Table 1 summarizes the half-inhibitory concentrations obtained for the three culture models. The XTT assay was used as the golden standard in the 2D culture and confirmed the caspase-3/7 results. The Caspase-Glo® 3/7 assay reveals an increase of chemoresistance between the 2D and the 3D cultures, although the comparison between the 2D and 3D conditions is delicate

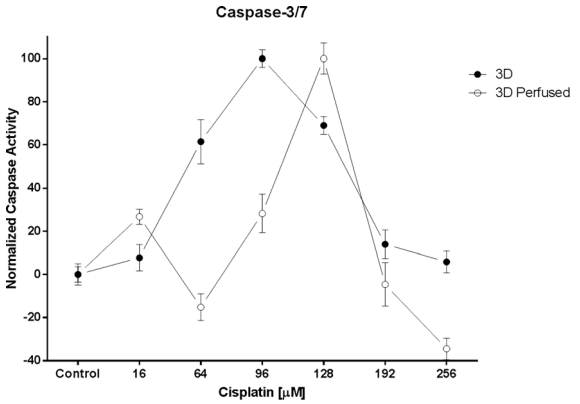

Fig. 6 The caspase-3/7 activity under 3D static (n = 3) and 3D perfused (n = 3) conditions. Data are presented as means ± SEM.

Table 1 Summary table of GI50 of cisplatin (μM) for the three conditions (2D, 3D and 3D perfused) obtained using two different viability assays (XTT and Caspase-Glo® 3/7)

Culture condition	XTT (μM)	Caspase-3/7 (μM)
2D	11	20
3D	—	54
3D perfused	—	105

due to the fact that cell density may influence the potency of toxic compounds.[37]

4. Conclusions

The present microfluidic device allows the individual entrapment of spheroids as well as their continuous perfusion. The morphology of the perfused spheroids is not affected by the dynamic environment and is similar to that of spheroids cultured under static conditions. Chemotherapeutic tests were performed on chip to evaluate the drug response of the perfused spheroids. A new technique, based on the collection and the analysis off chip of the supernatant using a standard plate reader, is demonstrated for the first time. The supernatant of only 8 spheroids is analyzed for cell apoptosis based on the Caspase-Glo® 3/7 assay. The use of a very small number of cells (about 5000 per assay) is of utmost importance, in particular for personalized medicine applications for which only a small number of cells from the patients' own tumor are available. Another advantage of this technique is clearly the very limited number of manipulations required to sample the supernatant and mix it with the Caspase-Glo® 3/7 reagent. In addition, the use of the supernatant, rather than the cells themselves, makes it possible to further investigate the spheroids using genomic and proteomic analysis or even histologic assessments of the spheroids. By perfusing the spheroids in this microfluidic system, it can be shown that MPM spheroids treated with cisplatin, one of the standard drugs used in the MPM therapy, were more chemoresistant than those in a static environment. This finding reveals the importance to better mimic the *in vivo* conditions found in MPM tumors, including the continuous delivery of nutrients and oxygen.

Acknowledgements

The authors wish to thank the Center for Micro-NanoTechnology (CMI) of the EPFL (Lausanne, Switzerland) for their help in the DRIE processing of the silicon wafers and Sandoz/Novartis, Switzerland, for providing the cisplatin. They are grateful to the Bernese Cancer League (Berne, Switzerland) and to the Novartis Foundation for medical-biological research (Switzerland) for funding this project. A special thank you also goes to the Johanna Dürmüller-Bol Foundation for providing financial support for the acquisition of several research instruments. Images were acquired on equipment supported by the Microscopy Imaging Center of the University of Berne.

References

1 F. Hirschhaeuser, H. Menne, C. Dittfeld, J. West, W. Mueller-Klieser and L. A. Kunz-Schughart, *J. Biotechnol.*, 2010, **148**, 3–15.
2 D. Barbone, T.-M. Yang, J. R. Morgan, G. Gaudino and V. C. Broaddus, *J. Biol. Chem.*, 2008, **283**, 13021–13030.
3 D. Barbone, J. A. Ryan, N. Kolhatkar, A. D. Chacko, D. M. Jablons, D. J. Sugarbaker, R. Bueno, A. G. Letai, L. M. Coussens, D. A. Fennell and V. C. Broaddus, *Cell Death Dis.*, 2011, **2**, e174.
4 K. M. Yamada and E. Cukierman, *Cell*, 2007, **130**, 601–610.
5 R. Derda, A. Laromaine, A. Mammoto, S. K. Y. Tang, T. Mammoto, D. E. Ingber and G. M. Whitesides, *Proc. Natl. Acad. Sci. U. S. A.*, 2009, **106**, 18457–18462.
6 J. Friedrich, R. Ebner and L. A. Kunz-Schughart, *Int. J. Radiat. Biol.*, **83**, 849–871.
7 L. Y. Wu, D. Di Carlo and L. P. Lee, *Biomed. Microdevices*, 2008, **10**, 197–202.
8 Z. Darzynkiewicz, E. Holden, A. Orfao, W. Telford, D. Wlodkowic, P. Lee, T. Gaige and P. Hung, *Methods Cell Biol.*, 2011, **102**, 77–103.
9 E. W. K. Young and D. J. Beebe, *Chem. Soc. Rev.*, 2010, **39**, 1036–1048.
10 J. El-Ali, P. K. Sorger and K. F. Jensen, *Nature*, 2006, **442**, 403–411.
11 D. Wlodkowic and J. M. Cooper, *Curr. Opin. Chem. Biol.*, 2010, **14**, 556–567.
12 Y. Morimoto and S. Takeuchi, *Biomater. Sci.*, 2013, **1**, 257.
13 K. Ziókowska, A. Stelmachowska, R. Kwapiszewski, M. Chudy, A. Dybko and Z. Brzózka, *Biosens. Bioelectron.*, 2013, **40**, 68–74.
14 A. Hsiao, Y.-S. Torisawa, Y. Tung, S. Sud, R. Taichman, K. Pienta and S. Takayama, *Biomaterials*, 2009, **30**, 3020–3027.
15 H. Ota and N. Miki, *Sens. Actuators, A*, 2011, **169**, 266–273.
16 L. Yu, M. C. W. Chen and K. C. Cheung, *Lab Chip*, 2010, **10**, 2424–2432.
17 T. Das, L. Meunier, L. Barbe, D. Provencher, O. Guenat, T. Gervais and A.-M. Mes-Masson, *Biomicrofluidics*, 2013, **7**, 011805.
18 S. Agastin, U.-B. T. Giang, Y. Geng, L. A. Delouise and M. R. King, *Biomicrofluidics*, 2011, **5**, 24110.

19 Y.-S. Torisawa, A. Takagi, Y. Nashimoto, T. Yasukawa, H. Shiku and T. Matsue, *Biomaterials*, 2007, **28**, 559–566.
20 J. Fukuda and K. Nakazawa, *Biomicrofluidics*, 2011, **5**, 022205.
21 C. Kim, J. H. Bang, Y. E. Kim, S. H. Lee and J. Y. Kang, *Lab Chip*, 2012, **12**, 4135–4142.
22 R. K. Goudar, *Ther. Clin. Risk Manage.*, 2008, **4**, 205–211.
23 M. Pistolesi and J. Rusthoven, *Chest*, 2004, **126**, 1318–1329.
24 D. E. Maziak, A. Gagliardi, A. E. Haynes, J. A. Mackay and W. K. Evans, *Lung Cancer*, 2005, **48**, 157–169.
25 R. M. Flores, H. I. Pass, V. E. Seshan, J. Dycoco, M. Zakowski, M. Carbone, M. S. Bains and V. W. Rusch, *J. Thorac. Cardiovasc. Surg.*, 2008, **135**, 620–626.
26 Y. T. Phung, D. Barbone, V. C. Broaddus and M. Ho, *J. Cancer*, 2011, **2**, 507–514.
27 W.-H. Tan and S. Takeuchi, *Proc. Natl. Acad. Sci. U. S. A.*, 2007, **104**, 1146–1151.
28 P. Valent, D. Bonnet, R. De Maria, T. Lapidot, M. Copland, J. V. Melo, C. Chomienne, F. Ishikawa, J. J. Schuringa, G. Stassi, B. Huntly, H. Herrmann, J. Soulier, A. Roesch, G. J. Schuurhuis, S. Wöhrer, M. Arock, J. Zuber, S. Cerny-Reiterer, H. E. Johnsen, M. Andreeff and C. Eaves, *Nat. Rev. Cancer*, 2012, **12**, 767–775.
29 B. J. Morrison, J. C. Steel and J. C. Morris, *PLoS One*, 2012, **7**, e49752.
30 L. Cortes-Dericks, G. L. Carboni, R. A. Schmid and G. Karoubi, *Gene Expression*, 2010, 437–444.
31 V. Levina, A. Marrangoni, T. Wang, S. Parikh, Y. Su, R. Herberman, A. Lokshin and E. Gorelik, *Cancer Res.*, 2010, **70**, 338–346.
32 D. B. Zamble and S. J. Lippard, *Trends Biochem. Sci.*, 1995, **20**, 435–439.
33 M. M. Tinnemans, B. Schutte, M. H. Lenders, G. P. Ten Velde, F. C. Ramaekers and G. H. Blijham, *Br. J. Cancer*, 1993, **67**, 1217–22.
34 A. Albanese, A. K. Lam, E. A. Sykes, J. V. Rocheleau and W. C. W. A. Chan, *Nat. Commun.*, 2013, **4**, 2718.
35 C. Godugu, A. R. Patel, U. Desai, T. Andey, A. Sams and M. Singh, *PLoS One*, 2013, **8**, e53708.
36 G. Hu and D. Li, *Biomed. Microdevices*, 2007, **9**, 315–23.
37 T. L. Riss and R. A. Moravec, *Assay Drug Dev. Technol.*, 2004, **2**, 51–62.